



Lack of effects of eight-week left dorsolateral prefrontal theta burst stimulation on white matter macro/microstructure and connection in autism

Chun-Hung Yeh^{1,2} · Po-Chun Lin² · Rung-Yu Tseng¹ · Yi-Ping Chao^{3,4} · Chen-Te Wu⁵ · Tai-Li Chou^{6,7,8} · Rou-Shayn Chen⁹ · Susan Shur-Fen Gau^{10,7} · Hsing-Chang Ni^{11,2} · Hsiang-Yuan Lin^{12,13}

Accepted: 8 March 2024 / Published online: 16 March 2024

© The Author(s), under exclusive licence to Springer Science+Business Media, LLC, part of Springer Nature 2024

Abstract

Whether brain stimulation could modulate brain structure in autism remains unknown. This study explored the impact of continuous theta burst stimulation (cTBS) over the left dorsolateral prefrontal cortex (DLPFC) on white matter macro/microstructure in intellectually able children and emerging adults with autism. Sixty autistic participants were randomized (30 active) and received active or sham cTBS for eight weeks twice per week, 16 total sessions using a double-blind (participant-, rater-, analyst-blinded) design. All participants received high-angular resolution diffusion MR imaging at baseline and week 8. Twenty-eight participants in the active group and twenty-seven in the sham group with good imaging quality entered the final analysis. With longitudinal fixel-based analysis and network-based statistics, we found no significant difference between the active and sham groups in changes of white matter macro/microstructure and connections following cTBS. In addition, we found no association between baseline white matter macro/microstructure and autistic symptom changes from baseline to week 8 in the active group. In conclusion, we did not find a significant impact of left DLPFC cTBS on white matter macro/microstructure and connections in children and emerging adults with autism. These findings need to be interpreted in the context that the current intellectually able cohort in a single university hospital site limits the generalizability. Future studies are required to investigate if higher stimulation intensities and/or doses, other personal factors, or rTMS parameters might confer significant brain structural changes visible on MRI in ASD.

Keywords Autism · Theta burst stimulation · Dorsolateral prefrontal cortex · Diffusion MRI · White matter

✉ Hsing-Chang Ni
alanni@cgmh.org.tw; alanni0918@yahoo.com.tw

¹ Department of Medical Imaging and Radiological Sciences, Chang Gung University, Taoyuan, Taiwan

² Department of Psychiatry, Chang Gung Memorial Hospital at Linkou, No.5 Fusing St. Gueishan, Taoyuan 333, Taiwan

³ Department of Computer Science and Information Engineering, Chang Gung University, Taoyuan, Taiwan

⁴ Department of Otorhinolaryngology-Head and Neck Surgery, Chang Gung Memorial Hospital at Linkou, Taoyuan, Taiwan

⁵ Department of Medical Imaging and Intervention, Chang Gung Memorial Hospital at Linkou, Taoyuan, Taiwan

⁶ Department of Psychology, National Taiwan University, Taipei, Taiwan

⁷ Graduate Institute of Brain and Mind Sciences, College of Medicine, National Taiwan University, Taipei, Taiwan

⁸ Neurobiology and Cognitive Science Center, National Taiwan University, Taipei, Taiwan

⁹ Department of Neurology, Chang Gung Memorial Hospital at Linkou, Taoyuan, Taiwan

¹⁰ Department of Psychiatry, National Taiwan University Hospital and College of Medicine, Taipei, Taiwan

¹¹ College of Medicine, Chang Gung University, Taoyuan, Taiwan

¹² Azrieli Adult Neurodevelopmental Centre, Campbell Family Mental Health Research Institute, Centre for Addiction and Mental Health, Toronto, ON, Canada

¹³ Department of Psychiatry, Temerty Faculty of Medicine, University of Toronto, Toronto, ON, Canada

Introduction

Autism spectrum disorder (ASD) is a neurodevelopmental disorder with which many individuals have long-term psychosocial functional challenges associated with social-communication deficits and repetitive/restricted behaviors (Lord et al., 2020). However, no biological intervention has been shown to reduce autistic symptoms.

Repetitive transcranial magnetic stimulation (rTMS), a non-invasive neuromodulation technique, can induce lasting brain activity change by stimulating the target region. rTMS has been applied in several neurological and psychiatric disorders with fair feasibility and safety (Lefaucheur et al., 2020). Theta burst stimulation (TBS), a modified rTMS variant, provides pulses in 50-Hz trains of three TMS pulses, repeated every 200 ms (Huang et al., 2005) with shorter stimulation duration and intensity than traditional rTMS (Huang et al., 2005; Schwippel et al., 2019). Although long-term potentiation and long-term depression after-effects of rTMS and TBS appear similar, whether the underlying neural mechanisms of rTMS and TBS are different or identical remains inconclusive (Li et al., 2019). Several clinical studies suggest that the therapeutic effects of TBS are comparable to rTMS. For example, Blumberger et al. (2018) have shown the efficacy of intermittent TBS is non-inferior to high-frequency (10 Hz) rTMS (considered a facilitatory role in many cortical regions) for neurotypical depression. Similarly, Li et al. (2022) have demonstrated similar efficacy between low-frequency (1 Hz) rTMS and continuous TBS (cTBS, primarily considered an inhibitory protocol) for neurotypical adults with generalized anxiety disorder. Given the shorter duration and lower seizure prevalence, TBS may be preferred for clinical practice (Schwippel et al., 2019).

The Excitatory/Inhibitory (E/I) imbalance hypothesis of ASD has been endorsed by altered gamma-aminobutyric acid (GABA) and glutamatergic functions (Masuda et al., 2019), increased glutamate concentration (Brown et al., 2013), reduced GABAergic interneurons activity (Buard et al., 2013), and reduced GABA levels (Schur et al., 2016) and receptors (Fatemi et al., 2009). rTMS could decrease rats' autistic-like behaviors by modulating E/I imbalance (Tan et al., 2018). Further, rTMS has been shown to stabilize hyperplasticity in autistic adults (Desarkar et al., 2021). These studies prompt the investigation of modulating E/I imbalance in ASD (Pietropaolo & Provenzano, 2022).

The dorsolateral prefrontal cortex (DLPFC) is a potential neuromodulation target for ASD (Cole et al., 2019). DLPFC plays essential roles in executive function (Friedman & Robbins, 2022), language processing (Hertrich et al., 2021), and emotion processing (Nejati et al., 2021),

whose dysfunction is associated with ASD. DLPFC function and structure are altered in ASD, including more neuron numbers (Courchesne et al., 2011), increased brain volumes (Carper & Courchesne, 2005), and hypoactivity (Carlisi et al., 2017). Based on the hypothesis that inhibiting cortical excitability may rectify E/I imbalance, Sokhadze et al. investigated inhibitory rTMS over the DLPFC in ASD, demonstrating beneficial potentials of DLPFC inhibitory rTMS for autistic repetitive behaviors (Casanova et al., 2012, 2014; Sokhadze et al., 2009, 2012, 2018). Nonetheless, this series of studies did not adopt randomization or sham-controlled design. Following this line of research based on the hypothesis of inhibitory rTMS for E/I imbalance, we conducted a double-blind sham-controlled randomized controlled trial (RCT) and found no significant impacts of DLPFC continuous TBS (cTBS) on core symptoms, emotion dysregulation and adaptive function in autistic youth (Ni et al., 2023b).

Prior neurotypical human studies suggest that rTMS/TBS-induced neuroplasticity occurs across brain systems and scales. For example, serum brain-derived neurotrophic factor (BDNF, a neurotrophin that regulates neuroplasticity at several scales (Kim et al., 2024)) levels increase following multiple-session rTMS in depression and anxiety (Lu et al., 2018; Zhao et al., 2019). These observed rTMS-induced serum BDNF increases may reflect increases in BDNF in the brain, which could have cascading effects on synaptic structure and function by modulating long-term potentiation (LTP)/long-term depression (LTD)-like processes (Kovalchuk et al., 2002). This alteration in BDNF and synapses may lead to altered release and binding of neurotransmitters (including dopamine, serotonin, gamma-aminobutyric acid [GABA], glutamate) following rTMS, which have been reported by rTMS trials combined with measurement of positron emission tomography/single photon emission computed tomography and magnetic resonance spectroscopy (MRS) across disorders (Fitzsimmons et al., 2023). Further, at the macro-scale level, studies using metrics based on electromyography or electroencephalography show increases in excitability and decreases in inhibition following high-frequency rTMS/iTBS (Fitzsimmons et al., 2023). Similar gains in regional function and function connectivity at the circuit level are also shown to correlate with clinical responses to high-frequency rTMS/iTBS in depression (M. Kirkovski et al., 2023a, 2023b). With long-term repeated modulation, these rTMS-induced network/circuit-level functional changes could finally lead to brain white matter (WM) changes (Sampaio-Baptista & Johansen-Berg, 2017; Scott & Frank, 2023), as evidenced in studies on stroke (Guo et al., 2016; Yang et al., 2015) and neurotypical depression (Ning et al., 2022).

Despite the neurotypical evidence for neuroplastic effects of rTMS/TBS, very limited studies have investigated rTMS/

TBS effects on brain structure and function in ASD. One recent magnetic resonance spectroscopy study found different local glutamate changes between active and sham DLPFC rTMS in autistic individuals (Moxon-Emre et al., 2021). However, our recent diffusion magnetic resonance imaging (dMRI) study did not find active vs. sham differences in WM macro/microstructural changes following 4-week intermittent TBS on posterior superior temporal sulci in autistic children and adolescents (Ni et al., 2023a). Since altered synaptic plasticity is believed to be essential pathophysiology of ASD (Bourgeron, 2015) and rTMS/TBS may modulate synaptic plasticity (Yang & Calakos, 2013), investigating rTMS/TBS effects on brain structure in ASD is crucial. Moreover, these findings may only be easily 'visible' by brain MRI (Godfrey et al., 2022).

As a companion to behavioral/clinical findings of our RCT (Ni et al., 2023b), this study investigated WM macro/microstructural and connection changes following MRI-navigated left DLPFC cTBS in intellectually able autistic children and emerging adults, with a double-blind sham-controlled design and a sufficiently powered sample. WM was characterized through fixel-based analysis (FBA) on dMRI data (Raffelt et al., 2017; Tournier et al., 2019). FBA assigns distinct quantitative metrics to an individual fiber population within each MRI voxel, referred to as 'fixel.' The derived fiber-specific metrics facilitate the quantification in both local microstructural fiber density and macroscopic cross-sectional area of fiber bundles, all at a fixel-wise level. FBA can investigate fiber-specific attributes, even within voxels comprising multiple fiber populations. This advantage elevates sensitivity and interpretability beyond conventional voxel-based analysis relying on voxel-averaged metrics (Raffelt et al., 2017). The autism-associated WM tract-specific alterations have been observed consistently using fixel-based analysis in previous studies. Specifically, Dimond et al. (2019) have reported lower fiber density across major WM pathways in autistic individuals. Kirkovski and colleagues have found sex-specific differences wherein autistic females exhibit reduced fiber density and cross-section in the corpus callosum (Kirkovski et al., 2020), and have revealed age-dependent WM changes in ASD, with younger individuals displaying more extensive alterations (Melissa Kirkovski et al., 2023a, 2023b). Our previous work has shown reductions in fixel metrics in ASD are predominantly seen in individuals with intellectual impairment, possibly exacerbated by minimal verbal expression (Yeh et al., 2022). A common thread across these previous studies was the consistent reduction in fixel-wise metrics (including fiber density, FD, fiber-bundle cross-section, FC, and FDC) in autistic individuals. A decrease in FD implies a reduction in intra-axonal volume fraction, indicating that the proportion of space occupied by axons diminishes within an imaging voxel. This could stem from either a decrease in axon

diameter or from fewer axons occupying this space (axonal loss). While both of these effects provide decreased capacity to transfer information, the current fixel-based analysis technique does not allow for the disentanglement of these two properties (Raffelt et al., 2017; Tournier et al., 2019).

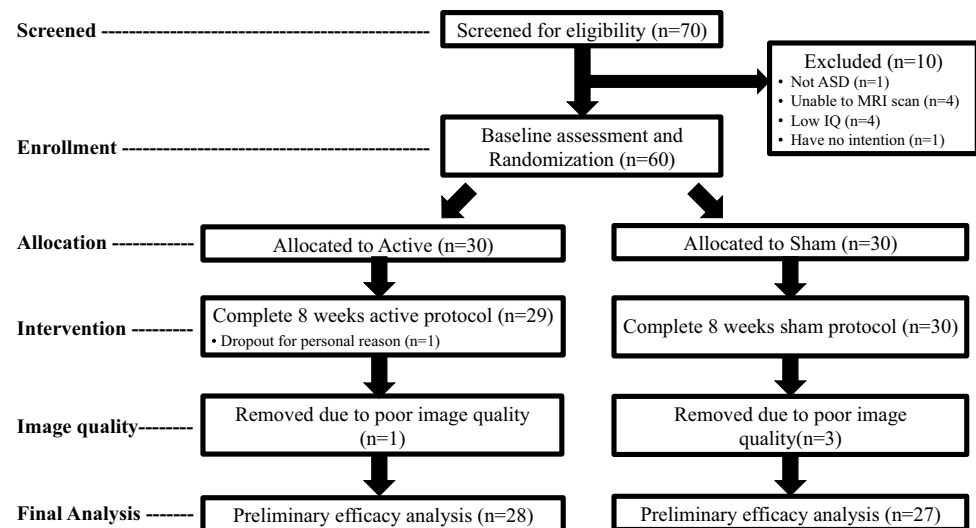
In addition, complementary to FBA, we assessed structural connectome using network-based statistics (NBS) (Zalesky et al., 2010). The non-parametric NBS method identifies pertinent subnetworks characterized by topologically linked connections. Using FBA and NBS, this study aimed to a) investigate potential alterations in WM structure and connections between active and sham cTBS in autistic individuals over an 8-week left DLPFC cTBS intervention; b) assess whether baseline WM would relate to autistic symptom changes following cTBS. We hypothesized that there would be alterations in the capability of information transfer due to cTBS-induced WM aberrations. Our approach was exploratory, employing whole-brain analysis to understand the influence of cTBS on WM. Given the scarce human empirical data, we did not make specific predictions regarding the involved circuitries and whether these effects would be positive or negative, acknowledging the need for further exploration into the effects of rTMS/TBS on WM in the absence of established hypotheses.

Methods

Design

This study was a parallel, double-blind (participant-, rater-, analyst-blinded), and sham-RCT of 8-week left DLPFC cTBS in autistic children and emerging adults. Autistic participants aged 8–30 were enrolled in a tertiary medical center in Taiwan between December 2019 and July 2022. Participants were randomized to either the active or sham group and received left DLPFC cTBS twice weekly for eight weeks (Fig. 1). During the study period, only the clinical assistants delivering cTBS intervention (operator) knew the Active/Sham allocation owing to the need to select the appropriate TMS coil for active or sham cTBS, but they were not involved in any outcome assessment and analysis. All of the clinical assistants had adequate training and received certification in delivering rTMS/TBS from the Taiwanese Society of Biological Psychiatry and Neuropsychopharmacology before they were allowed to provide rTMS/TBS stimulations. Participants, their parents, the research staff who administered the social cognition tasks and the principal investigator (parents, staff, and PI were raters) were all blind to the Active/Sham allocation until the last outcome assessment was completed in Week 12. Our blinding processes identically followed the standard adopted by all of the previous double-blind rTMS RCTs in autistic people (Ameis

Fig. 1 Flowchart of clinical trial and diffusion MRI data quality assurance



et al., 2020; Enticott et al., 2014, 2021) and most RCTs in neurotypical adults with depression (Blumberger et al., 2016; Fitzgerald et al., 2012) and schizophrenia (Voineskos et al., 2021). A research statistician, independent of the study implementation and blind to the allocation, completed all statistical analyses after the trial completion. Details are reported elsewhere (Ni et al., 2023b).

Our trial was approved by the Research Ethics Committee at the hospital (201802246A0) and registered with ClinicalTrials.gov (NCT04993144). Informed consent was obtained from participants and their parents. All study procedures adhere to the 1964 Helsinki Declaration and its later amendments or comparable ethical standards.

Participants

Participants (aged 8–30 years) were clinically diagnosed with ASD, further confirmed by the Autism Diagnosis Objective Schedule (Chang et al., 2023). We excluded participants with a full-scale intelligence quotient < 70 based on the Wechsler Intelligence Scale-IV for Children or Adults, any history of major neurological or systemic illness, or any lifetime diagnosis of major psychiatric disorders, including mood and anxiety disorders, schizophrenia, or substance use. Participants with co-occurring attention-deficit/hyperactivity disorder ($n = 36$) were included. During the trial, all psychiatric medications stayed the same. All participants had been naïve to any neuromodulation.

Intervention

Sixty participants were randomized (30 active). The biphasic pulses for TBS were generated with the Magstim Super Rapid² system (Magstim Company, Oxford, UK) and applied with the 70-mm figure-of-eight coil. Initially, we placed the

coil tangentially to the scalp over the contralateral motor cortex with the handle pointing backward. The location of the motor “hot-spot” was determined where single-pulse TMS produced the largest motor-evoked potentials (MEPs) from the first dorsal interosseus (FDI) muscle. We measured the active motor threshold (AMT) as the minimum stimulation intensity needed to elicit MEPs of no less than 200 μV in 5 out of 10 trials during 20% of maximum voluntary contraction of the FDI. Later, the coil was placed on the individual’s DLPFC, which was transformed from MNI coordinates (-42.5, 31.7, 41.4) to individual T1-weighted native space, using the Navigated Brain Stimulation system (Nexstim®, Helsinki, Finland) (Lacadie et al., 2008; Mylius et al., 2013; Ni et al., 2017). The coil was oriented approximately 45° to the sagittal plane of the head, with the coil handle pointing posteriorly.

The active DLPFC stimulation comprised the intensity of 90% active motor threshold. The sham adopted the same intensity, with a sham coil producing tactile and auditory stimulation without direct brain effects. The average of individual AMT (ranging from 39 to 90%) was 59 with a standard deviation of 11. Notably, the scalp-to-cortex distance differences between the motor cortex and DLPFC and stimulation intensities are both individual, likely resulting in heterogeneous TBS dosing. Therefore, we used SimNIBS v3.2 (Saturnino et al., 2019) to model the individual normalized induced electric field over the DLPFC (Fig. 2). For the tissue segmentation and volumetric meshing, we followed the previous method and used “headreco” combined with CAT12 (Caulfield et al., 2021). “Headreco” segmented each participant’s T1-weighted anatomical MRI and created a volumetric mesh combing the tissue layers into a 3D model. The default vertex density of “headreco” is 0.5 nodes per mm^2 . The head meshes contained an average of 619,689 nodes ($\text{SD} = 47,025$, range = 497,693–826,589), 884,443 triangles

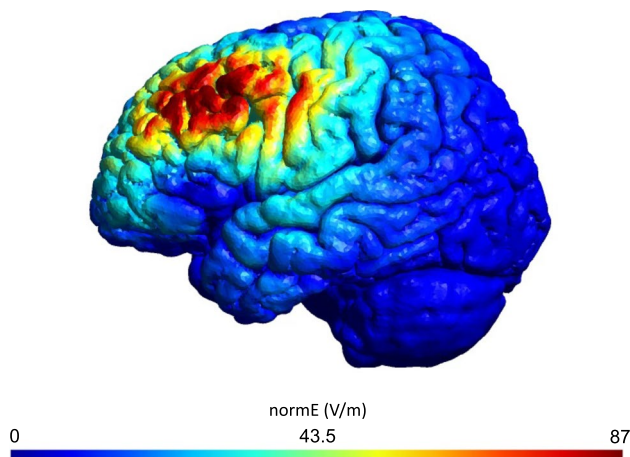


Fig. 2 Model of the normalized electric field (normE) induced by cTBS over the left dorsolateral prefrontal cortex in a given participant. The coordinates of the left dorsolateral prefrontal cortex were translated from MNI (-42.5, 31.7, 41.4) to native space of this exemplary participant. Models were computed using SimNIBS 3.2 (Saturnino et al., 2019) based on the study's protocol and default parameters in SimNIBS 3.2

(SD = 67,032, range = 731,582–1,145,156) and 3,445,388 tetrahedra (SD = 263,773, range = 2,778,834–4,615,565). Then we did the quality control via careful visual inspection and Z-score determination to exclude volume outliers (Caulfield, Badran, DeVries, et al., 2020; Caulfield, Badran, Li, et al., 2020a, 2020b). The ratio between normalized induced fields (V/m) of left DLPFC and motor cortex was calculated for each participant and used as a covariate for all statistical analyses. Individualized induced electric field was detailed in the Supplementary Note. The cTBS protocol comprised a burst of 3 TMS pulses at 50 Hz at 200 ms intervals for continuous 40 s (600 pulses/course) for each course (Ni et al., 2023b).

MRI scans

Each participant underwent an MRI scan at baseline (t_1) and Week 8 (t_2). Data were acquired on a 3 Tesla GE Discovery MR750 scanner with an 8-channel head coil. Anatomical T1-weighted images (T1WIs) were collected using the inversion-recovery spoiled gradient-echo (GE's BRAVO) sequence, with 156 axial slices scanned at TR/TE = 8.2/3.2 ms, inversion time = 450 ms, flip angle = 12°, matrix size = 256 × 256, in-plane resolution = 1.0 mm, and slice thickness = 1.0 mm. High-angular resolution dMRI data were collected using a single-shot spin-echo diffusion-weighted echo-planar imaging sequence: 2.3-mm isotropic voxel, TR/TE = 7500/83 ms, matrix size = 96 × 96, 128 diffusion directions at b-value = 2000s/mm², and 10 b = 0 volumes.

MRI preprocessing

The dMRI preprocessing pipeline encompassed several established methods, including denoising (Cordero-Grande et al., 2019), Gibbs ring removal (Kellner et al., 2016), correction for image distortion (Schilling et al., 2020), inter-volume movement (Jenkinson et al., 2012), bias field (Tustison et al., 2010), and upsampling. Following preprocessing, quality control was assessed using FSL (Bastiani et al., 2019) and visual inspection to identify potential issues. A data quality index was defined per the percentage of total outliers in dMRI data. This index indicates the proportion of image volumes exhibiting excessive signal loss. Data with artifacts or excessive in-scanner motion (average root-mean-square (RMS) between-volume displacements, relative RMS, > 1 mm) were excluded. Following preprocessing and quality control, 55 participants (28 active) were included in the longitudinal analysis (Fig. 1).

For all preprocessed t_1 dMRI data, tissue response functions were estimated using an unsupervised algorithm (Dhollander et al., 2019). For both t_1 and t_2 data, fiber orientation distributions (FODs) were reconstructed based on constrained spherical deconvolution (Tournier et al., 2008) by modeling the presence of WM and cerebrospinal fluid compartments via group-averaged response functions using the multi-tissue framework (Jeurissen et al., 2014). Finally, intensity normalization was applied to address the compartmental inhomogeneities (Tournier et al., 2019).

Longitudinal FBA

Fixel template & metrics

Group fixel template: Within each participant, rigid registration was performed to align the t_1 and t_2 FOD images, followed by transformations of FODs at both time points to a common intermediate space (the participant's mid-way space). The transformed t_1 - t_2 FODs were then averaged to create intra-participant mean FODs. Using per-participant mean FODs, an inter-participant group FOD template was constructed, serving as a representative spatial reference for fiber orientations across all participants in the longitudinal dataset (Raffelt et al., 2017). The group FOD template was subjected to a segmentation process to identify distinct fixels within the template FODs (Smith et al., 2013).

Longitudinal fixel metrics: To align an individual's fixels at each time point with the group template fixels, a FOD-guided registration process was conducted (Raffelt et al., 2017). Then for each participant at each time point, standard fixel-wise metrics were computed, including FD (measuring intra-axonal volume), FC (measuring macroscopic/volumetric changes in the entire local fiber bundle), FDC (providing

a holistic assessment of connectivity by incorporating both microscopic FD and macroscopic FC) (Raffelt et al., 2017). These fixel-wise metrics computed for all participants, and time points were projected onto the corresponding fixels of the group template. Furthermore, to quantify changes from the baseline t_1 to t_2 , two longitudinal fixel metrics were calculated:

$$\Delta FD_{actual} = FD_{t_2} - FD_{t_1} \quad (1)$$

$$\Delta FD_{relative} = \Delta FD_{actual} / FD_{t_1} \quad (2)$$

Equations (1) and (2) were actual and relative differences in FD, respectively. The same approach was adapted for FC and FDC, with the distinction that FC was subjected to a logarithmic transformation before calculating these longitudinal measures.

Fixel-wise statistics

The statistical analysis of whole-brain fixel-wise metrics was performed using a general linear model alongside the connectivity-based fixel enhancement (CFE) approach (Raffelt et al., 2015). To enable CFE, a whole-brain tractogram was generated on the FOD template and then post-processed with SIFT (Smith et al., 2013). This tractogram was employed to compute fixel-to-fixel connectivity, which enabled fixel data smoothing and enhanced statistics (Raffelt et al., 2015).

The following analyses were conducted to examine the cTBS effects:

- *Between-group comparisons:* We assessed the Treatment-by-Time effect to determine whether active-sham differences existed in longitudinal fixel metrics.
- *Within-group pairwise comparisons:* Longitudinal fixel metrics were evaluated within each treatment from t_1 to t_2 .
- *Brain-symptom relationships:* Autistic social-communication symptoms were gauged using the Social Responsiveness Scale (SRS). The relative alteration of SRS ($\Delta SRS_{relative} = (SRS_{t_2} - SRS_{t_1}) / SRS_{t_1}$) from t_1 to t_2 was computed. We examined whether $\Delta SRS_{relative}$ related to the standard FBA metrics at t_1 . This algorithm was executed identically for repetitive/restricted behaviors estimated by the Repetitive Behaviors Scale–Revised (RBS-R).

The nuisance variables included age, in-scanner head motion (quantified by relative RMS displacement; averaged if modeling two time points), intracranial volume, and SimNIBS ratio. The significance was determined using a family-wise error-corrected P-value ($P_{FWE} < 0.05$). Non-parametric

testing involving 20,000 permutations would yield a more precise estimate of the error within each test.

Structural connectome

Connectome construction

A tractography-based connectome was generated in native space as follows:

- *Brain parcellation:* Schaefer’s cortical atlas (100 regions) (Schaefer et al., 2017), Tien’s subcortical parcellation (50 regions) (Tian et al., 2020), and SUIT’s cerebellum atlas (34 regions) (Diedrichsen et al., 2011) were integrated into a parcellation scheme.
- *Image registration:* T1WIs were initially registered to the preprocessed mean $b=0$ images via a rigid-body transformation (FSL’s FLIRT) (Jenkinson et al., 2012). Further registration was performed between the individual’s T1WI and MNI 152 template, employing both linear and non-linear warps through ANTs (<http://stnava.github.io/ANTs/>). The resulting warp fields were utilized to map the parcellation images from the MNI space to the native space via an inverse transformation.
- *Fiber tracking:* Anatomically-constrained tractography (Smith et al., 2012) was performed to generate whole-brain probabilistic tractograms of 100 million streamlines using the dynamic seeding approach (Smith et al., 2015) and the recommended algorithm and parameters of MRtrix3 (Tournier et al., 2019).
- *Tractogram quantification:* SIFT2 was applied to modulate the contribution weight of each streamline, respecting the underlying fiber density (Smith et al., 2015).
- *Connectome generation:* Structural connectomes were constructed by assigning the SIFT2-modulated streamline weights to the nearest node via searching from the streamline endpoint (Yeh et al., 2019). The edge weight of each connection was defined as the sum of the relevant SIFT2 streamline weights, essentially representing a *weighted* streamline count.

NBS

A repeated-measures analysis of variance of edge-wise connectivity was performed using NBS (Zalesky et al., 2010), examining the main effects of time, treatment, and their interactions. Networks were permuted 10,000 times to obtain an empirical null distribution to control for FWE across a substantial number of connectome edges, with a significance threshold at $P_{FWE} < 0.05$ applied to a height threshold of $t = 3.0$. This t threshold corresponded to $P = 0.002$. This thresholding process yielded a weighted connectivity

matrix comprising suprathreshold connections, controlling for the preceding nuisance regressors.

Results

The demographic data (Table 1) was all compatible between the two groups. The individual normalized induced electric field ranged 97–149% of DLPFC relative to the motor cortex (Table S1), with no between-group difference.

Baseline

The active group showed greater baseline microstructural FD at the body and isthmus of the corpus callosum than the sham ($P_{FWE} < 0.05$; number of fixels = 276; Fig. 3). There were no significant between-group baseline disparities in FC and FDC.

Using NBS, between-group differences (active > sham) of three subnetworks were identified at baseline (Fig. 4). These left-lateralized networks encompassed the following brain regions: a) caudate, cuneus, and lingual gyrus ($P_{FWE} = 0.0002$); b) precentral and superior frontal gyrus, and putamen ($P_{FWE} = 0.0002$); c) caudate and middle frontal gyrus ($P_{FWE} = 0.002$).

Following cTBS

Using either actual or relative longitudinal FBA metrics per group, we did not find significant Treatment-by-Time interaction. Furthermore, baseline WM macro/microstructure did not relate to autistic symptom changes. Likewise, no NBS results achieved any statistical significance.

Discussion

We used complementary approaches (FBA and NBS connectome) to investigate 8-week DLPFC cTBS effects on WM in intellectually able autistic children and emerging adults. Corresponding to our clinical findings (Ni et al., 2023b), the current cTBS protocol did not induce WM macro/microstructural and connection changes in ASD. Further, we did not find baseline WM features related to symptom changes following cTBS. Baseline differences in FBA and connectome subnetworks were observed. This is a justifiable phenomenon because a random artifact could exist despite proper randomization, as implemented herein (Altman, 1985).

In the autistic population, the present study and our previous work (Ni et al., 2023a), despite null results from both studies, are the first few endeavors investigating the impacts

Table 1 Demographics and baseline characteristics of participants with autism spectrum disorder of the adequate diffusion MRI data quality across baseline and week 8

	Active (n = 28)	Sham (n = 27)	P value
Age (years), mean (S.D.)	13.0 (3.4)	13.1 (2.8)	0.767
Male, n (%)	26 (92.9)	24 (88.9)	0.670
RMS _{1l} (mm), mean (S.D.)	0.268 (0.092)	0.307 (0.151)	0.447
Total outliers _{1l} (%), mean (S.D.)	0.65 (0.68)	0.59 (0.64)	0.781
RMS ₁₂ (mm), mean (S.D.)	0.298 (0.114)	0.310 (0.169)	0.940
Total outliers ₁₂ (%), mean (S.D.)	0.63 (0.56)	0.67 (0.88)	0.444
ICV _{1l} (cm ³), mean (S.D.)	1594.1 (106.2)	1556.1 (139.3)	0.398
Intelligence quotient (IQ), mean (S.D.)			
Full intelligence	86.5 (17.5)	87.8 (17.9)	0.960
Verbal Comprehension index	88.4 (20.0)	87.6 (15.4)	0.939
Perceptual Reasoning Index	91.8 (19.1)	92.6 (20.5)	0.888
Working Memory Index	92.5 (17.4)	88.9 (15.3)	0.554
Processing Speed Index	80.4 (15.3)	79.4 (15.6)	0.636
Social Responsiveness Scale, mean (S.D.)	109.8 (28.6)	112.7 (24.9)	0.696
Repetitive Behavior Scale-Revised, mean (S.D.)	38.1 (23.8)	38.0 (26.4)	0.893
NormE (DLPFC/motor)	1.2 (0.1)	1.2 (0.1)	0.297
Comorbidity with ADHD, n (%)	18 (64.3)	18 (66.7)	0.853
Medication, n (%)			
Methylphenidate	12 (42.9)	14 (51.9)	0.504
Psychotherapy, n (%)	5 (17.9)	8 (29.6)	0.304

Acronyms: S.D. – standard deviation; RMS – relative Root-Mean-Square framewise displacement during diffusion MRI; ICV – Intra-Cranial Volume

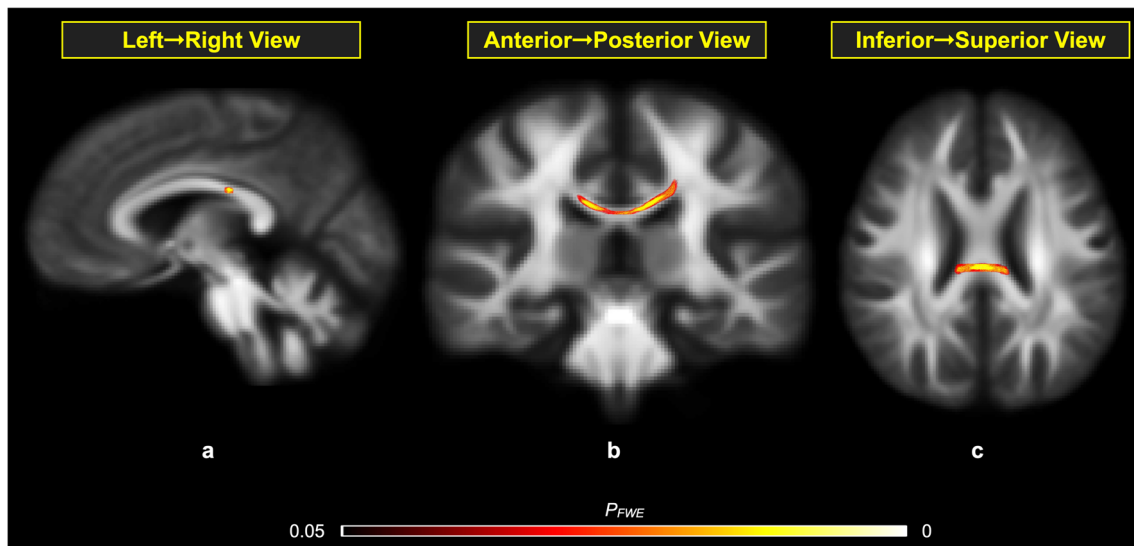


Fig. 3 Results of between-group comparisons from the fixel-based analysis at the baseline assessment (a: left–right view; b: anterior–posterior view; c: inferior–superior view). White matter tract seg-

ments having significant group differences in FD are displayed and colored by the family-wise error corrected P -value (P_{FWE})

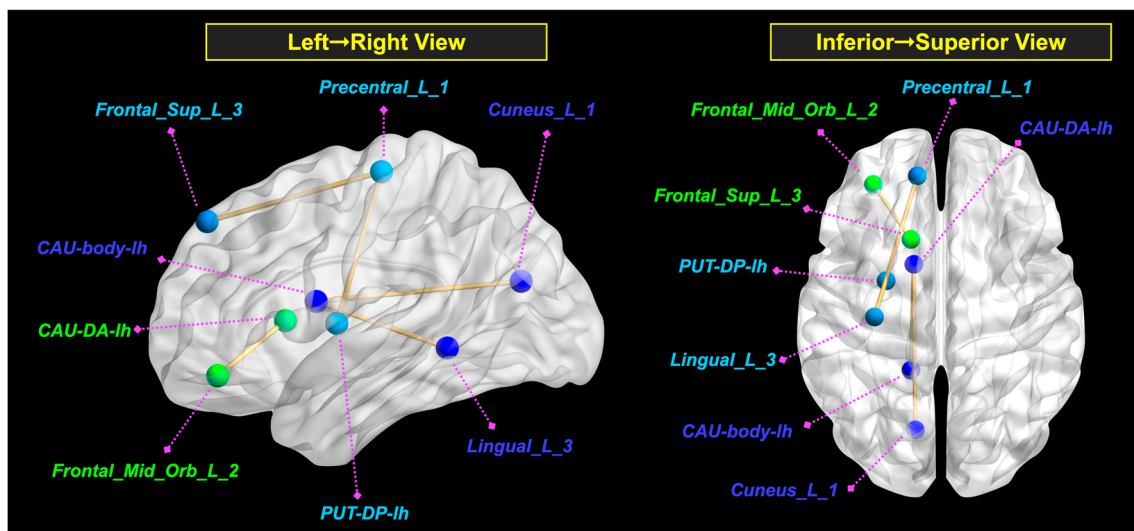


Fig. 4 Results of between-group comparisons from the network-based statistics at the baseline assessment (left: left–right view; right: inferior–superior view). Brain regions are represented by spheres, with colors denoting distinct networks. Abbreviations – CAU-body-lh: body of the caudate nucleus; Lingual_L_3: lingual gyrus;

Precentral_L_1: precentral gyrus; Frontal_Sup_L_3: superior frontal gyrus; PUT-DP-lh: dorsal posterior putamen; CAU-DA-lh: dorsal anterior caudate nucleus; Frontal_Mid_Orb_L_2: orbital section of middle frontal gyrus. L or lh indicates the left hemisphere

of rTMS/TBS on WM. Similarly, there is limited evidence from animal studies (Seewoo et al., 2022) and human studies on stroke (Ueda et al., 2019; Yamada et al., 2018; Yang et al., 2015), which show the neuroplastic effect of TBS on WM microstructural properties. Specifically, the prior pre-clinical study on the animal model of depression has shown that 10 Hz low-intensity rTMS could rescue abnormal WM by increasing myelination in young male rats (Seewoo et al.,

2022). In humans, low-frequency rTMS over the nonlesional hemisphere plus intensive occupation therapy can increase white matter microstructural integrity for both the lesional and nonlesional primary motor cortex (Yamada et al., 2018) and enhance WM information flow (Ueda et al., 2019). cTBS also has been shown to improve microstructural properties across several WM tracts in patients with stroke (Yang et al., 2015). On the other hand, evidence from functional

MRI and MRS studies in the neurotypical population shows neuroplasticity occurs across brain networks and scales. Taking cTBS as an example, cTBS can have inhibitory effects on neuropsychological function and neural networks (Lasagna et al., 2021). For example, cTBS would impair working memory (targeting DLPFC) (Vekony et al., 2018) and conscious olfactory perception (targeting right orbitofrontal cortex) (Villafuerte et al., 2019). A recent MRS study indicates that cTBS could modulate GABA level changes and is linked with the interhemispheric inhibition (Matsuta et al., 2022; Stoby et al., 2022). Resting-state functional MRI studies show brain intrinsic functional connectivity generally decreases in response to cTBS and increases in response to iTBS (Cohan et al., 2023; M. Kirkovski et al., 2023a, 2023b), which endorses the assumption of LTP and LTD-like plasticity effects of iTBS and cTBS, respectively. Taken together, the extant neurotypical literature endorses the neuroplasticity effects of multi-session rTMS/TBS. The use of other modalities will provide a more complete picture and advance a nuanced understanding of the complex neurobiological effects of rTMS/TBS in autism.

Consistent with our previous study (Ni et al., 2023a), we found a lack of impacts of 8-week DLPFC cTBS on WM, which may be explained by the following reasons. First, the optimal stimulation dosing is inconclusive (Cocchi et al., 2023). The current stimulation frequency is lower than the protocol for depression (van Rooij et al., 2023). This frequency was decided considering the feasibility and was compatible with previous open-label trials of DLPFC rTMS in ASD (Casanova et al., 2012, 2014; Sokhadze et al., 2009, 2012, 2018). Further, we delivered 600 pulses per cTBS session in the present study. Based on our previous trial in ASD (Ni et al., 2021), the original protocol planned to adopt 1,200 pulses per session, which was requested by the Taiwanese FDA to be modified into the current intensity eventually because of safety considerations. Together with our previous study (Ni et al., 2023a), the cumulative dose of 9,600 total pulses may not be enough to induce neuroplasticity, which could be 'visible' as WM changes. Second, we only targeted the left DLPFC, decided based on the consensus statement (Cole et al., 2019). Although targeting bilateral DLPFC might arguably enhance efficacy (Sokhadze et al., 2018), most of the evidence, especially in depression, suggests stimulating left and right DLPFC could generate distinct effects, respectively. To avoid potential counteraction, we targeted the left side only. Third, cTBS aftereffects might be idiosyncratic in ASD. Namely, Jannati et al. (2020) demonstrated more than half of 11 autistic children had a facilitatory response to M1 cTBS, while most neurotypical youth showed 'ordinary' inhibitory aftereffects. Later, Jannati et al. (2021) found consistent post-cTBS inhibitory effects in autistic adults ($n = 19$). This post-cTBS idiosyncrasy might average out as the null result at a group level. Lastly, ASD

as an early-onset neurodevelopmental condition of synaptic dysfunction (i.e., synaptopathies origin early in life) (Bourgeron, 2015) may have altered aftereffects involved in the mechanism underpinning rTMS-induced plasticity (Oberman & Benussi, 2023), engendering the insensitivity of autistic brain to change. This speculation may account for the inconsistency that rTMS is associated with WM changes in depression (acquiring dysfunctional plasticity later in life) (Peng et al., 2012; Tateishi et al., 2019), while no such effect is observed in schizophrenia (Voineskos et al., 2021), another disorder of developmental synaptopathology (Calabrese et al., 2016).

This study has some limitations. First, the range of participants' ages was wide (8–30 years). Previous preliminary studies suggest age may moderate the after-effect of cTBS in autistic people (Oberman & Benussi, 2023). Although the current distribution of participants' ages was similar to previous studies of low-frequency rTMS in autistic individuals (Baruth et al., 2010; Casanova et al., 2012, 2014; Sokhadze et al., 2010, 2012, 2009, 2018, 2014a, 2014b) and we included age as a covariate, the wide age range may still introduce some confounding effects. Second, to facilitate the feasibility of recruitment and generalization of the findings to 'real-world' autistic populations, we included autistic youth with common psychiatric comorbidities (e.g., anxiety and ADHD) and psychiatric medications. How comorbidities/medications, after-effects of rTMS/TBS, and white matter morphometry would interact remains unknown. Third, this study did not adopt a sex-balanced recruitment strategy, despite the sex-stratified randomization. Given the fact that assigned sex at birth may have effects on the autistic brain (Walsh et al., 2021), the sex effect on the after-effect of rTMS/TBS in autism awaits future investigations. In addition to the limitations and issues discussed above, methodological variability in stimulation parameters, protocols, participant diagnosis, and demographic factors across studies make the objective of whether/how rTMS/TBS could modulate white matter inconclusive. More multimodal and multi-time point research is necessary to fully delineate the effect of TBS on structure, function, and metabolites in gray and white matter in healthy and disordered brains in the future.

Conclusion

Our MRI-guided DLPFC cTBS intervention failed to induce WM changes in autistic children and emerging adults. These findings need to be interpreted in the context that the current intellectually able cohort in a single university hospital site limits the generalizability. Future studies are required to investigate if higher stimulation

intensities and/or doses, other personal factors, or rTMS parameters might confer significant brain structural changes visible on MRI in ASD.

Supplementary Information The online version contains supplementary material available at <https://doi.org/10.1007/s11682-024-00874-x>.

Acknowledgements The authors would like to thank all of our participants and their family members for partaking in this study and the anonymous reviewers for comments that significantly improved the manuscript. We want to pay tribute to the late Professor Ying-Zu Huang, who guided and inspired this study with wisdom, insight, and tenacity.

Author Contributions All authors read and approved the final manuscript. Conceptualization and design: Hsing-Chang Ni, Hsiang-Yuan Lin; Methodology: Yi-Ping Chao, Chen-Te Wu, Rou-Shayn Chen, Chun-Hung Yeh; Clinical data collection: Hsing-Chang Ni; Neuroimaging data collection: Hsing-Chang Ni, Yi-Ping Chao, Chen-Te Wu; Formal analysis: Hsiang-Chang Ni, Rung-Yu Tseng, Chun-Hung Yeh, Hsiang-Yuan Lin; Interpretation: Hsiang-Chang Ni, Po-Chun Lin, Chun-Hung Yeh, and Hsiang-Yuan Lin; Writing—original draft preparation: Hsiang-Chang Ni, Po-Chun Lin, Chun-Hung Yeh, and Hsiang-Yuan Lin; Figures: Hsiang-Chang Ni, Rung-Yu Tseng, Chun-Hung Yeh; Writing—review and editing: All authors; Funding acquisition: Hsing-Chang Ni; Resources: Tai-Li Chou and Susan Shur-Fen Gau; Supervision: Hsiang-Yuan Lin.

Funding This work is supported by grants from the Ministry of Science and Technology of Taiwan (108–2628-B-182A-006–; 109–2628-B-182A-010–; 110–2628-B-182A-016–; 112–2221-E-182–029). Hsiang-Yuan Lin is supported by the Azrieli Adult Neurodevelopmental Centre at Centre for Addiction and Mental Health, and an Academic Scholar Award from the Department of Psychiatry, University of Toronto. The funders had no role in the study's design, in the collection, analyses, or interpretation of data, in the writing of the manuscript, or in the decision to publish the results.

Data availability The datasets generated during and/or analyzed during the current study are available from the corresponding author upon reasonable request.

Declarations

Competing interests The authors declare no competing interests.

Ethics approval All procedures performed in studies involving human participants were in accordance with the ethical standards of the institutional research committee and with the 1964 Helsinki Declaration and its later amendments or comparable ethical standards. The Research Ethics Committee approved the study at Chang Gung Memorial Hospital, Linkou, Taiwan (201802246A0), and registered with ClinicalTrials.gov (NCT04993144).

Consent to participate All participants provided informed consent.

Consent for publication All participants provided informed consent to publish the data.

Conflict of interests All authors have no financial or non-financial interests relevant to the content of this article to disclose.

References

- Altman, D. G. (1985). Comparability of Randomised Groups. *Journal of the Royal Statistical Society. Series D (The Statistician)*, 34(1), 125–136.
- Ameis, S. H., Blumberger, D. M., Croarkin, P. E., Mabbott, D. J., Lai, M. C., Desarkar, P., . . . Daskalakis, Z. J. (2020). Treatment of Executive Function Deficits in autism spectrum disorder with repetitive transcranial magnetic stimulation: A double-blind, sham-controlled, pilot trial. *Brain Stimul*, 13(3), 539–547. <https://doi.org/10.1016/j.brs.2020.01.007>
- Baruth, J. M., Casanova, M. F., El-Baz, A., Horrell, T., Mathai, G., Sears, L., & Sokhadze, E. (2010). Low-Frequency Repetitive Transcranial Magnetic Stimulation (rTMS) Modulates Evoked-Gamma Frequency Oscillations in Autism Spectrum Disorder (ASD). *Journal of Neurotherapy*, 14(3), 179–194. <https://doi.org/10.1080/10874208.2010.501500>
- Bastiani, M., Cottaar, M., Fitzgibbon, S. P., Suri, S., Alfaro-Almagro, F., Sotiropoulos, S. N., . . . Andersson, J. L. R. (2019). Automated quality control for within and between studies diffusion MRI data using a non-parametric framework for movement and distortion correction. *Neuroimage*, 184, 801–812. <https://doi.org/10.1016/j.neuroimage.2018.09.073>
- Blumberger, D. M., Maller, J. J., Thomson, L., Mulsant, B. H., Rajji, T. K., Maher, M., . . . Daskalakis, Z. J. (2016). Unilateral and bilateral MRI-targeted repetitive transcranial magnetic stimulation for treatment-resistant depression: a randomized controlled study. *J Psychiatry Neurosci*, 41(4), E58–66. <https://doi.org/10.1503/jpn.150265>
- Blumberger, D. M., Vila-Rodriguez, F., Thorpe, K. E., Feffer, K., Noda, Y., Giacobbe, P., . . . Downar, J. (2018). Effectiveness of theta burst versus high-frequency repetitive transcranial magnetic stimulation in patients with depression (THREE-D): a randomised non-inferiority trial. *Lancet*, 391(10131), 1683–1692. [https://doi.org/10.1016/S0140-6736\(18\)30295-2](https://doi.org/10.1016/S0140-6736(18)30295-2)
- Bourgeron, T. (2015). From the genetic architecture to synaptic plasticity in autism spectrum disorder. *Nature Reviews Neuroscience*, 16(9), 551–563. <https://doi.org/10.1038/nrn3992>
- Brown, M. S., Singel, D., Hepburn, S., & Rojas, D. C. (2013). Increased glutamate concentration in the auditory cortex of persons with autism and first-degree relatives: A (1)H-MRS study. *Autism Research*, 6(1), 1–10. <https://doi.org/10.1002/aur.1260>
- Buard, I., Rogers, S. J., Hepburn, S., Kronberg, E., & Rojas, D. C. (2013). Altered oscillation patterns and connectivity during picture naming in autism. *Frontiers in Human Neuroscience*, 7, 742. <https://doi.org/10.3389/fnhum.2013.00742>
- Calabrese, F., Riva, M. A., & Molteni, R. (2016). Synaptic alterations associated with depression and schizophrenia: Potential as a therapeutic target. *Expert Opinion on Therapeutic Targets*, 20(10), 1195–1207. <https://doi.org/10.1080/14728222.2016.1188080>
- Carlisi, C. O., Norman, L. J., Lukito, S. S., Radua, J., Mataix-Cols, D., & Rubia, K. (2017). Comparative Multimodal Meta-analysis of Structural and Functional Brain Abnormalities in Autism Spectrum Disorder and Obsessive-Compulsive Disorder. *Biological Psychiatry*, 82(2), 83–102. <https://doi.org/10.1016/j.biopsych.2016.10.006>
- Carper, R. A., & Courchesne, E. (2005). Localized enlargement of the frontal cortex in early autism. *Biological Psychiatry*, 57(2), 126–133. <https://doi.org/10.1016/j.biopsych.2004.11.005>
- Casanova, M. F., Baruth, J. M., El-Baz, A., Tasman, A., Sears, L., & Sokhadze, E. (2012). Repetitive Transcranial Magnetic Stimulation (rTMS) Modulates Event-Related Potential (ERP) Indices of Attention in Autism. *Translational Neuroscience*, 3(2), 170–180. <https://doi.org/10.2478/s13380-012-0022-0>

- Casanova, M. F., Hensley, M. K., Sokhadze, E. M., El-Baz, A. S., Wang, Y., Li, X., & Sears, L. (2014). Effects of weekly low-frequency rTMS on autonomic measures in children with autism spectrum disorder. *Frontiers in Human Neuroscience*, 8, 851. <https://doi.org/10.3389/fnhum.2014.00851>
- Caulfield, K. A., Badran, B. W., Li, X., Bikson, M., & George, M. S. (2020b). Can transcranial electrical stimulation motor threshold estimate individualized tDCS doses over the prefrontal cortex? Evidence from reverse-calculation electric field modeling. *Brain Stimulation*, 13(4), 1150–1152. <https://doi.org/10.1016/j.brs.2020.05.012>
- Caulfield, K. A., Li, X., & George, M. S. (2021). A reexamination of motor and prefrontal TMS in tobacco use disorder: Time for personalized dosing based on electric field modeling? *Clinical Neurophysiology*, 132(9), 2199–2207. <https://doi.org/10.1016/j.clinph.2021.06.015>
- Caulfield, K. A., Badran, B. W., DeVries, W. H., Summers, P. M., Kofmehl, E., Li, X., . . . George, M. S. (2020). Transcranial electrical stimulation motor threshold can estimate individualized tDCS dosage from reverse-calculation electric-field modeling. *Brain Stimul*, 13(4), 961–969. <https://doi.org/10.1016/j.brs.2020.04.007>
- Chang, J. C., Lai, M. C., Chien, Y. L., Cheng, C. Y., Wu, Y. Y., & Gau, S. S. (2023). Psychometric properties of the Mandarin version of the autism diagnostic observation Schedule-Generic. *Journal of the Formosan Medical Association*, 122(7), 574–583. <https://doi.org/10.1016/j.jfma.2023.01.008>
- Cocchi, L., Naze, S., Robinson, C., Webb, L., Sonkusare, S., Hearne, L. J., . . . Breakspear, M. (2023). Effects of transcranial magnetic stimulation of the rostromedial prefrontal cortex in obsessive–compulsive disorder: a randomized clinical trial. *Nature Mental Health*, 1(8), 555–563. <https://doi.org/10.1038/s44220-023-00094-0>
- Cohan, R., Rafique, S. A., Stoby, K. S., Gorbet, D. J., & Steeves, J. K. E. (2023). Continuous and intermittent theta burst stimulation of primary visual cortex do not modulate resting state functional connectivity: A sham-controlled multi-echo fMRI study. *Brain and Behavior: A Cognitive Neuroscience Perspective*, 13(5), e2989. <https://doi.org/10.1002/brb3.2989>
- Cole, E. J., Enticott, P. G., Oberman, L. M., Gwynette, M. F., Casanova, M. F., Jackson, S. L. J., . . . T. M. S. i. A. S. D. C. G. (2019). The Potential of Repetitive Transcranial Magnetic Stimulation for Autism Spectrum Disorder: A Consensus Statement. *Biol Psychiatry*, 85(4), e21–e22. <https://doi.org/10.1016/j.biopsych.2018.06.003>
- Cordero-Grande, L., Christiaens, D., Hutter, J., Price, A. N., & Hajnal, J. V. (2019). Complex diffusion-weighted image estimation via matrix recovery under general noise models. *NeuroImage*, 200, 391–404. <https://doi.org/10.1016/j.neuroimage.2019.06.039>
- Courchesne, E., Mouton, P. R., Calhoun, M. E., Semendeferi, K., Ahrens-Barbeau, C., Hallet, M. J., . . . Pierce, K. (2011). Neuron number and size in prefrontal cortex of children with autism. *JAMA*, 306(18), 2001–2010. <https://doi.org/10.1001/jama.2011.1638>
- Desarkar, P., Rajji, T. K., Ameis, S. H., Blumberger, D. M., Lai, M. C., Lunskey, Y., & Daskalakis, Z. J. (2021). Assessing and stabilizing atypical plasticity in autism spectrum disorder using rTMS: Results from a proof-of-principle study. *Clinical Neurophysiology*. <https://doi.org/10.1016/j.clinph.2021.03.046>
- Dhollander, T., Mito, R., Raffelt, D., & Connelly, A. (2019). Improved white matter response function estimation for 3-tissue constrained spherical deconvolution. In: Proc. Intl. Soc. Mag. Reson. Med. (p. 555). ISMRM.
- Diedrichsen, J., Maderwald, S., Küper, M., Thürling, M., Rabe, K., Gizewski, E. R., . . . Timmann, D. (2011). Imaging the deep cerebellar nuclei: A probabilistic atlas and normalization procedure. *Neuroimage*, 54(3), 1786–1794. <https://doi.org/10.1016/j.neuroimage.2010.10.035>
- Dimond, D., Schuetze, M., Smith, R. E., Dhollander, T., Cho, I., Vinette, S., . . . Bray, S. (2019). Reduced white matter fiber density in autism spectrum disorder. *Cerebral Cortex*, 29(4), 1778–1788. <https://doi.org/10.1093/cercor/bhy348>
- Enticott, P. G., Fitzgibbon, B. M., Kennedy, H. A., Arnold, S. L., Elliot, D., Peachey, A., . . . Fitzgerald, P. B. (2014). A double-blind, randomized trial of deep repetitive transcranial magnetic stimulation (rTMS) for autism spectrum disorder. *Brain Stimulation*, 7(2), 206–211. <https://doi.org/10.1016/j.brs.2013.10.004>
- Enticott, P. G., Barlow, K., Guastella, A. J., Licari, M. K., Rogasch, N. C., Middeldorp, C. M., . . . Fitzgerald, P. B. (2021). Repetitive transcranial magnetic stimulation (rTMS) in autism spectrum disorder: protocol for a multicentre randomised controlled clinical trial. *BMJ Open*, 11(7), e046830. <https://doi.org/10.1136/bmjopen-2020-046830>
- Fatemi, S. H., Reutiman, T. J., Folsom, T. D., & Thuras, P. D. (2009). GABA(A) receptor downregulation in brains of subjects with autism. *Journal of Autism and Developmental Disorders*, 39(2), 223–230. <https://doi.org/10.1007/s10803-008-0646-7>
- Fitzgerald, P. B., Hoy, K. E., Herring, S. E., McQueen, S., Peachey, A. V., Segrave, R. A., . . . Daskalakis, Z. J. (2012). A double blind randomized trial of unilateral left and bilateral prefrontal cortex transcranial magnetic stimulation in treatment resistant major depression. *J Affect Disord*, 139(2), 193–198. <https://doi.org/10.1016/j.jad.2012.02.017>
- Fitzsimmons, S. M. D. D., Oostra, E., Postma, T. S., van der Werf, Y. D., & van den Heuvel, O. A. (2023). Repetitive Transcranial Magnetic Stimulation-Induced Neuroplasticity and the Treatment of Psychiatric Disorders: State of the Evidence and Future Opportunities. *Biological Psychiatry*. <https://doi.org/10.1016/j.biopsych.2023.11.016>
- Friedman, N. P., & Robbins, T. W. (2022). The role of prefrontal cortex in cognitive control and executive function. *Neuropsychopharmacology*, 47(1), 72–89. <https://doi.org/10.1038/s41386-021-01132-0>
- Godfrey, K. E. M., Muthukumaraswamy, S. D., Steiner, C. M., & Hoeh, N. (2022). Decreased salience network fMRI functional connectivity following a course of rTMS for treatment-resistant depression. *Journal of Affective Disorders*, 300, 235–242. <https://doi.org/10.1016/j.jad.2021.12.129>
- Guo, Z., Jin, Y., Peng, H., Xing, G., Liao, X., Wang, Y., . . . Mu, Q. (2016). Ipsilesional High Frequency Repetitive Transcranial Magnetic Stimulation Add-On Therapy Improved Diffusion Parameters of Stroke Patients with Motor Dysfunction: A Preliminary DTI Study. *Neural Plast*, 2016, 6238575. <https://doi.org/10.1155/2016/6238575>
- Hertrich, I., Dietrich, S., Blum, C., & Ackermann, H. (2021). The Role of the Dorsolateral Prefrontal Cortex for Speech and Language Processing. *Frontiers in Human Neuroscience*, 15, 645209. <https://doi.org/10.3389/fnhum.2021.645209>
- Huang, Y. Z., Edwards, M. J., Rounis, E., Bhatia, K. P., & Rothwell, J. C. (2005). The burst stimulation of the human motor cortex. *Neuron*, 45(2), 201–206. <https://doi.org/10.1016/j.neuron.2004.12.033>
- Jannati, A., Ryan, M. A., Block, G., Kayarian, F. B., Oberman, L. M., Rotenberg, A., & Pascual-Leone, A. (2021). Modulation of motor cortical excitability by continuous theta-burst stimulation in adults with autism spectrum disorder. *Clinical Neurophysiology*, 132(7), 1647–1662. <https://doi.org/10.1016/j.clinph.2021.03.021>
- Jannati, A., Block, G., Ryan, M. A., Kaye, H. L., Kayarian, F. B., Bashir, S., . . . Rotenberg, A. (2020). Continuous Theta-Burst Stimulation in Children With High-Functioning Autism

- Spectrum Disorder and Typically Developing Children. *Front Integr Neurosci*, 14, 13. <https://doi.org/10.3389/fnint.2020.00013>
- Jenkinson, M., Beckmann, C. F., Behrens, T. E. J., Woolrich, M. W., & Smith, S. M. (2012). *FSL. Neuroimage*, 62(2), 782–790. <https://doi.org/10.1016/j.neuroimage.2011.09.015>
- Jeurissen, B., Tournier, J. D., Dhollander, T., Connelly, A., & Sijbers, J. (2014). Multi-tissue constrained spherical deconvolution for improved analysis of multi-shell diffusion MRI data. *NeuroImage*, 103, 411–426. <https://doi.org/10.1016/j.neuroimage.2014.07.061>
- Kellner, E., Dhital, B., Kiselev, V. G., & Reiser, M. (2016). Gibbs-ringing artifact removal based on local subvoxel-shifts. *Magnetic Resonance in Medicine*, 76(5), 1574–1581. <https://doi.org/10.1002/mrm.26054>
- Kim, J., He, M. J., Widmann, A. K., & Lee, F. S. (2024). The role of neurotrophic factors in novel, rapid psychiatric treatments. *Neuropsychopharmacology*, 49(1), 227–245. <https://doi.org/10.1038/s41386-023-01717-x>
- Kirkovski, M., Donaldson, P. H., Do, M., Speranza, B. E., Albein-Urios, N., Oberman, L. M., & Enticott, P. G. (2023a). A systematic review of the neurobiological effects of theta-burst stimulation (TBS) as measured using functional magnetic resonance imaging (fMRI). *Brain Structure & Function*, 228(3–4), 717–749. <https://doi.org/10.1007/s00429-023-02634-x>
- Kirkovski, M., Fuelscher, I., Hyde, C., Donaldson, P. H., Ford, T. C., Rossell, S. L., . . . Enticott, P. G. (2020). Fixel based analysis reveals atypical white matter micro- and macrostructure in adults with autism spectrum disorder: An investigation of the role of biological sex. *Frontiers in Integrative Neuroscience*, 14. <https://doi.org/10.3389/fnint.2020.00040>
- Kirkovski, M., Singh, M., Dhollander, T., Fuelscher, I., Hyde, C., Albein-Urios, N., . . . Enticott, P. G. (2023). An Investigation of Age-related Neuropathophysiology in Autism Spectrum Disorder Using Fixel-based Analysis of Corpus Callosum White Matter Micro- and Macrostructure. *Journal of Autism and Developmental Disorders*. <https://doi.org/10.1007/s10803-023-05980-1>
- Kovalchuk, Y., Hanse, E., Kafitz, K. W., & Konnerth, A. (2002). Post-synaptic Induction of BDNF-Mediated Long-Term Potentiation. *Science*, 295(5560), 1729–1734. <https://doi.org/10.1126/science.1067766>
- Lacadie, C. M., Fulbright, R. K., Rajeevan, N., Constable, R. T., & Papademetris, X. (2008). More accurate Talairach coordinates for neuroimaging using non-linear registration. *NeuroImage*, 42(2), 717–725. <https://doi.org/10.1016/j.neuroimage.2008.04.240>
- Lasagna, C. A., Taylor, S. F., Lee, T. G., Rutherford, S., Greathouse, T., Gu, P., & Tso, I. F. (2021). Continuous Theta Burst Stimulation to the Secondary Visual Cortex at 80% Active Motor Threshold Does Not Impair Central Vision in Humans During a Simple Detection Task. *Frontiers in Human Neuroscience*, 15, 709275. <https://doi.org/10.3389/fnhum.2021.709275>
- Lefaucheur, J. P., Aleman, A., Baeken, C., Benninger, D. H., Brunelin, J., Di Lazzaro, V., . . . Ziemann, U. (2020). Evidence-based guidelines on the therapeutic use of repetitive transcranial magnetic stimulation (rTMS): An update (2014–2018). *Clin Neurophysiol*, 131(2), 474–528. <https://doi.org/10.1016/j.clinph.2019.11.002>
- Li, C. T., Huang, Y. Z., Bai, Y. M., Tsai, S. J., Su, T. P., & Cheng, C. M. (2019). Critical role of glutamatergic and GABAergic neurotransmission in the central mechanisms of theta-burst stimulation. *Human Brain Mapping*, 40(6), 2001–2009. <https://doi.org/10.1002/hbm.24485>
- Li, X., Zhang, C., Tan, J., Ding, L., Wang, C., Wang, M., & Lin, Y. (2022). Clinical effects of continuous theta burst stimulation for generalized anxiety disorder and a mechanism involving alpha oscillations: a randomized controlled trial. *Journal of Psychiatry & Neuroscience*, 47(2), E123–E133. <https://doi.org/10.1503/jpn.210134>
- Lord, C., Brugha, T. S., Charman, T., Cusack, J., Dumas, G., Frazier, T., . . . Veenstra-VanderWeele, J. (2020). Autism spectrum disorder. *Nat Rev Dis Primers*, 6(1), 5. <https://doi.org/10.1038/s41572-019-0138-4>
- Lu, R., Zhang, C., Liu, Y., Wang, L., Chen, X., & Zhou, X. (2018). The effect of bilateral low-frequency rTMS over dorsolateral prefrontal cortex on serum brain-derived neurotrophic factor and serotonin in patients with generalized anxiety disorder. *Neuroscience Letters*, 684, 67–71. <https://doi.org/10.1016/j.neulet.2018.07.008>
- Masuda, F., Nakajima, S., Miyazaki, T., Yoshida, K., Tsugawa, S., Wada, M., . . . Noda, Y. (2019). Motor cortex excitability and inhibitory imbalance in autism spectrum disorder assessed with transcranial magnetic stimulation: a systematic review. *Transl Psychiatry*, 9(1), 110. <https://doi.org/10.1038/s41398-019-0444-3>
- Matsuta, H., Shimomura, T., Kouchiyama, T., & Fujiki, M. (2022). Continuous theta-burst stimulation to the sensorimotor cortex affects contralateral gamma-aminobutyric acid level and resting-state networks. *PLoS ONE*, 17(8), e0272268. <https://doi.org/10.1371/journal.pone.0272268>
- Moxon-Emre, I., Daskalakis, Z. J., Blumberger, D. M., Croarkin, P. E., Lyon, R. E., Forde, N. J., . . . Ameis, S. H. (2021). Modulation of Dorsolateral Prefrontal Cortex Glutamate/Glutamine Levels Following Repetitive Transcranial Magnetic Stimulation in Young Adults With Autism. *Front Neurosci*, 15, 711542. <https://doi.org/10.3389/fnins.2021.711542>
- Mylus, V., Ayache, S. S., Ahdab, R., Farhat, W. H., Zouari, H. G., Belke, M., . . . Lefaucheur, J. P. (2013). Definition of DLPFC and M1 according to anatomical landmarks for navigated brain stimulation: inter-rater reliability, accuracy, and influence of gender and age. *NeuroImage*, 78, 224–232. <https://doi.org/10.1016/j.neuroimage.2013.03.061>
- Nejati, V., Majidi, R., Salehinejad, M. A., & Nitsche, M. A. (2021). The role of dorsolateral and ventromedial prefrontal cortex in the processing of emotional dimensions. *Science and Reports*, 11(1), 1971. <https://doi.org/10.1038/s41598-021-81454-7>
- Ni, H. C., Hung, J., Wu, C. T., Wu, Y. Y., Chang, C. J., Chen, R. S., & Huang, Y. Z. (2017). The Impact of Single Session Intermittent Theta-Burst Stimulation over the Dorsolateral Prefrontal Cortex and Posterior Superior Temporal Sulcus on Adults with Autism Spectrum Disorder. *Frontiers in Neuroscience*, 11, 255. <https://doi.org/10.3389/fnins.2017.00255>
- Ni, H. C., Chen, Y. L., Chao, Y. P., Wu, C. T., Wu, Y. Y., Liang, S. H., . . . Lin, H. Y. (2021). Intermittent theta burst stimulation over the posterior superior temporal sulcus for children with autism spectrum disorder: A 4-week randomized blinded controlled trial followed by another 4-week open-label intervention. *Autism*, 25(5), 1279–1294. <https://doi.org/10.1177/1362361321990534>
- Ni, H. C., Chao, Y. P., Tseng, R. Y., Wu, C. T., Cocchi, L., Chou, T. L., . . . Lin, H. Y. (2023a). Lack of effects of four-week theta burst stimulation on white matter macro/microstructure in children and adolescents with autism. *NeuroImage Clin*, 37, 103324. <https://doi.org/10.1016/j.nicl.2023.103324>
- Ni, H. C., Chen, Y. L., Chao, Y. P., Wu, C. T., Chen, R. S., Chou, T. L., . . . Lin, H. Y. (2023b). A lack of efficacy of continuous theta burst stimulation over the left dorsolateral prefrontal cortex in autism: A double blind randomized sham-controlled trial. *Autism Res*, 16(6), 1247–1262. <https://doi.org/10.1002/aur.2954>
- Ning, L., Rathi, Y., Barbour, T., Makris, N., & Camprodon, J. A. (2022). White matter markers and predictors for subject-specific rTMS response in major depressive disorder. *Journal of Affective Disorders*, 299, 207–214. <https://doi.org/10.1016/j.jad.2021.12.005>

- Oberman, L. M., & Benussi, A. (2023). Transcranial magnetic stimulation across the lifespan: Impact of developmental and degenerative processes. *Biological Psychiatry*. <https://doi.org/10.1016/j.biopsych.2023.07.012>
- Peng, H., Zheng, H., Li, L., Liu, J., Zhang, Y., Shan, B., . . . Zhang, Z. (2012). High-frequency rTMS treatment increases white matter FA in the left middle frontal gyrus in young patients with treatment-resistant depression. *J Affect Disord*, *136*(3), 249–257. <https://doi.org/10.1016/j.jad.2011.12.006>
- Pietropaolo, S., & Provenzano, G. (2022). Editorial: Targeting excitation-inhibition imbalance in neurodevelopmental and autism spectrum disorders. *Frontiers in Neuroscience*, *16*, 968115. <https://doi.org/10.3389/fnins.2022.968115>
- Raffelt, D. A., Tournier, J. D., Smith, R. E., Vaughan, D. N., Jackson, G., Ridgway, G. R., & Connelly, A. (2017). Investigating white matter fibre density and morphology using fixel-based analysis. *NeuroImage*, *144*(Pt A), 58–73. <https://doi.org/10.1016/j.neuroimage.2016.09.029>
- Raffelt, D. A., Smith, R. E., Ridgway, G. R., Tournier, J. D., Vaughan, D. N., Rose, S., . . . Connelly, A. (2015). Connectivity-based fixel enhancement: Whole-brain statistical analysis of diffusion MRI measures in the presence of crossing fibres. *Neuroimage*, *117*, 40–55. <https://doi.org/10.1016/j.neuroimage.2015.05.039>
- Sampaio-Baptista, C., & Johansen-Berg, H. (2017). White Matter Plasticity in the Adult Brain. *Neuron*, *96*(6), 1239–1251. <https://doi.org/10.1016/j.neuron.2017.11.026>
- Saturnino, G. B., Puonti, O., Nielsen, J. D., Antonenko, D., Madsen, K. H., & Thielscher, A. (2019). SimNIBS 2.1: A Comprehensive Pipeline for Individualized Electric Field Modelling for Transcranial Brain Stimulation. In S. Makarov, M. Horner, & G. Noetscher (Eds.), *Brain and Human Body Modeling: Computational Human Modeling at EMBC 2018* (pp. 3–25). https://doi.org/10.1007/978-3-030-21293-3_1
- Schaefer, A., Kong, R., Gordon, E. M., Laumann, T. O., Zuo, X.-N., Holmes, A. J., . . . Yeo, B. T. T. (2017). Local-Global Parcellation of the Human Cerebral Cortex from Intrinsic Functional Connectivity MRI. *Cerebral Cortex*, *28*(9), 3095–3114. <https://doi.org/10.1093/cercor/bhx179>
- Schilling, K. G., Blaber, J., Hansen, C., Cai, L., Rogers, B., Anderson, A. W., . . . Landman, B. A. (2020). Distortion correction of diffusion weighted MRI without reverse phase-encoding scans or field-maps. *PLOS ONE*, *15*(7), e0236418. <https://doi.org/10.1371/journal.pone.0236418>
- Schur, R. R., Draisma, L. W., Wijnen, J. P., Boks, M. P., Koevoets, M. G., Joels, M., . . . Vinkers, C. H. (2016). Brain GABA levels across psychiatric disorders: A systematic literature review and meta-analysis of (1) H-MRS studies. *Hum Brain Mapp*, *37*(9), 3337–3352. <https://doi.org/10.1002/hbm.23244>
- Schwippel, T., Schroeder, P. A., Fallgatter, A. J., & Plewnia, C. (2019). Clinical review: The therapeutic use of theta-burst stimulation in mental disorders and tinnitus. *Progress in Neuro-Psychopharmacology and Biological Psychiatry*, *92*, 285–300. <https://doi.org/10.1016/j.pnpb.2019.01.014>
- Scott, D. N., & Frank, M. J. (2023). Adaptive control of synaptic plasticity integrates micro- and macroscopic network function. *Neuropsychopharmacology*, *48*(1), 121–144. <https://doi.org/10.1038/s41386-022-01374-6>
- Seewoo, B. J., Feindel, K. W., Won, Y., Joos, A. C., Figliomeni, A., Hennessy, L. A., & Rodger, J. (2022). White Matter Changes Following Chronic Restraint Stress and Neuromodulation: A Diffusion Magnetic Resonance Imaging Study in Young Male Rats. *Biol Psychiatry Glob Open Sci*, *2*(2), 153–166. <https://doi.org/10.1016/j.bpsgos.2021.08.006>
- Smith, R. E., Tournier, J.-D., Calamante, F., & Connelly, A. (2012). Anatomically-constrained tractography: Improved diffusion MRI streamlines tractography through effective use of anatomical information. *NeuroImage*, *62*(3), 1924–1938. <https://doi.org/10.1016/j.neuroimage.2012.06.005>
- Smith, R. E., Tournier, J.-D., Calamante, F., & Connelly, A. (2013). SIFT: Spherical-deconvolution informed filtering of tractograms. *NeuroImage*, *67*, 298–312. <https://doi.org/10.1016/j.neuroimage.2012.11.049>
- Smith, R. E., Tournier, J. D., Calamante, F., & Connelly, A. (2015). SIFT2: Enabling dense quantitative assessment of brain white matter connectivity using streamlines tractography. *NeuroImage*, *119*, 338–351. <https://doi.org/10.1016/j.neuroimage.2015.06.092>
- Sokhadze, E. M., El-Baz, A., Baruth, J., Mathai, G., Sears, L., & Casanova, M. F. (2009). Effects of low frequency repetitive transcranial magnetic stimulation (rTMS) on gamma frequency oscillations and event-related potentials during processing of illusory figures in autism. *Journal of Autism and Developmental Disorders*, *39*(4), 619–634. <https://doi.org/10.1007/s10803-008-0662-7>
- Sokhadze, E. M., El-Baz, A. S., Sears, L. L., Opris, I., & Casanova, M. F. (2014a). rTMS neuromodulation improves electrocortical functional measures of information processing and behavioral responses in autism. *Frontiers in Systems Neuroscience*, *8*, 134. <https://doi.org/10.3389/fnsys.2014.00134>
- Sokhadze, E. M., El-Baz, A. S., Tasman, A., Sears, L. L., Wang, Y., Lamina, E. V., & Casanova, M. F. (2014b). Neuromodulation integrating rTMS and neurofeedback for the treatment of autism spectrum disorder: An exploratory study. *Applied Psychophysiology and Biofeedback*, *39*(3–4), 237–257. <https://doi.org/10.1007/s10484-014-9264-7>
- Sokhadze, E. M., Lamina, E. V., Casanova, E. L., Kelly, D. P., Opris, I., Tasman, A., & Casanova, M. F. (2018). Exploratory Study of rTMS Neuromodulation Effects on Electrocortical Functional Measures of Performance in an Oddball Test and Behavioral Symptoms in Autism. *Frontiers in Systems Neuroscience*, *12*, 20. <https://doi.org/10.3389/fnsys.2018.00020>
- Sokhadze, E., Baruth, J., Tasman, A., Mansoor, M., Ramaswamy, R., Sears, L., . . . Casanova, M. F. (2010). Low-frequency repetitive transcranial magnetic stimulation (rTMS) affects event-related potential measures of novelty processing in autism. *Applied Psychophysiology and Biofeedback*, *35*(2), 147–161. <https://doi.org/10.1007/s10484-009-9121-2>
- Sokhadze, E. M., Baruth, J. M., Sears, L., Sokhadze, G. E., El-Baz, A. S., & Casanova, M. F. (2012). Prefrontal neuromodulation using rTMS improves error monitoring and correction function in autism. *Applied Psychophysiology and Biofeedback*, *37*(2), 91–102. <https://doi.org/10.1007/s10484-012-9182-5>
- Stoby, K. S., Rafique, S. A., Oeltzschner, G., & Steeves, J. K. E. (2022). Continuous and intermittent theta burst stimulation to the visual cortex do not alter GABA and glutamate concentrations measured by magnetic resonance spectroscopy. *Brain and Behavior: A Cognitive Neuroscience Perspective*, *12*(2), e2478. <https://doi.org/10.1002/brb3.2478>
- Tan, T., Wang, W., Xu, H., Huang, Z., Wang, Y. T., & Dong, Z. (2018). Low-Frequency rTMS Ameliorates Autistic-Like Behaviors in Rats Induced by Neonatal Isolation Through Regulating the Synaptic GABA Transmission. *Frontiers in Cellular Neuroscience*, *12*, 46. <https://doi.org/10.3389/fncel.2018.00046>
- Tateishi, H., Nishihara, M., Kawaguchi, A., Matsushima, J., Murakawa, T., Haraguchi, Y., . . . Monji, A. (2019). Improvement Of Frontal Lobe Dysfunction And White Matter Integrity By rTMS In Treatment-Resistant Depression. *Neuropsychiatr Dis Treat*, *15*, 3079–3087. <https://doi.org/10.2147/NDT.S228501>
- Tian, Y., Margulies, D. S., Breakspear, M., & Zalesky, A. (2020). Topographic organization of the human subcortex unveiled with functional connectivity gradients. *Nature Neuroscience*, *23*(11), 1421–1432. <https://doi.org/10.1038/s41593-020-00711-6>

- Tournier, J. D., Yeh, C. H., Calamante, F., Cho, K. H., Connelly, A., & Lin, C. P. (2008). Resolving crossing fibres using constrained spherical deconvolution: Validation using diffusion-weighted imaging phantom data. *NeuroImage*, 42(2), 617–625. <https://doi.org/10.1016/j.neuroimage.2008.05.002>
- Tournier, J. D., Smith, R., Raffelt, D., Tabbara, R., Dhollander, T., Pietsch, M., . . . Connelly, A. (2019). MRtrix3: A fast, flexible and open software framework for medical image processing and visualisation. *Neuroimage*, 202, 116137. <https://doi.org/10.1016/j.neuroimage.2019.116137>
- Tustison, N. J., Avants, B. B., Cook, P. A., Zheng, Y., Egan, A., Yushkevich, P. A., & Gee, J. C. (2010). N4ITK: Improved N3 Bias Correction. *IEEE Transactions on Medical Imaging*, 29(6), 1310–1320. <https://doi.org/10.1109/TMI.2010.2046908>
- Ueda, R., Yamada, N., Abo, M., & Senoo, A. (2019). Relationship between motor function improvements and white matter structure after low-frequency repetitive transcranial magnetic stimulation plus intensive occupational therapy in chronic subcortical stroke patients. *NeuroReport*, 30(7), 485–490. <https://doi.org/10.1097/WNR.0000000000001227>
- van Rooij, S. J. H., Arulpragasam, A. R., McDonald, W. M., & Philip, N. S. (2023). Accelerated TMS - moving quickly into the future of depression treatment. *Neuropsychopharmacology*. <https://doi.org/10.1038/s41386-023-01599-z>
- Vekony, T., Nemeth, V. L., Holczer, A., Kocsis, K., Kincses, Z. T., Vecsei, L., & Must, A. (2018). Continuous theta-burst stimulation over the dorsolateral prefrontal cortex inhibits improvement on a working memory task. *Science and Reports*, 8(1), 14835. <https://doi.org/10.1038/s41598-018-33187-3>
- Villafuerte, G., Miguel-Puga, A., & Arias-Carrion, O. (2019). Continuous Theta Burst Stimulation Over the Right Orbitofrontal Cortex Impairs Conscious Olfactory Perception. *Frontiers in Neuroscience*, 13, 555. <https://doi.org/10.3389/fnins.2019.00555>
- Voineskos, A. N., Blumberger, D. M., Schifani, C., Hawco, C., Dickie, E. W., Rajji, T. K., . . . Daskalakis, Z. J. (2021). Effects of Repetitive Transcranial Magnetic Stimulation on Working Memory Performance and Brain Structure in People With Schizophrenia Spectrum Disorders: A Double-Blind, Randomized, Sham-Controlled Trial. *Biol Psychiatry Cogn Neurosci Neuroimaging*, 6(4), 449–458. <https://doi.org/10.1016/j.bpsc.2020.11.011>
- Walsh, M. J. M., Wallace, G. L., Gallegos, S. M., & Braden, B. B. (2021). Brain-based sex differences in autism spectrum disorder across the lifespan: A systematic review of structural MRI, fMRI, and DTI findings. *NeuroImage: Clinical*, 31, 102719. <https://doi.org/10.1016/j.nicl.2021.102719>
- Yamada, N., Ueda, R., Kakuda, W., Momosaki, R., Kondo, T., Hada, T., . . . Abo, M. (2018). Diffusion Tensor Imaging Evaluation of Neural Network Development in Patients Undergoing Therapeutic Repetitive Transcranial Magnetic Stimulation following Stroke. *Neural Plast*, 2018, 3901016. <https://doi.org/10.1155/2018/3901016>
- Yang, Y., & Calakos, N. (2013). *Presynaptic Long-Term Plasticity*. *Front Synaptic Neurosci*, 5, 8. <https://doi.org/10.3389/fnsyn.2013.00008>
- Yang, W., Liu, T. T., Song, X. B., Zhang, Y., Li, Z. H., Cui, Z. H., . . . Liu, J. (2015). Comparison of different stimulation parameters of repetitive transcranial magnetic stimulation for unilateral spatial neglect in stroke patients. *J Neurol Sci*, 359(1–2), 219–225. <https://doi.org/10.1016/j.jns.2015.08.1541>
- Yeh, C.-H., Smith, R. E., Dhollander, T., Calamante, F., & Connelly, A. (2019). Connectomes from streamlines tractography: Assigning streamlines to brain parcellations is not trivial but highly consequential. *NeuroImage*, 199, 160–171. <https://doi.org/10.1016/j.neuroimage.2019.05.005>
- Yeh, C.-H., Tseng, R.-Y., Ni, H.-C., Cocchi, L., Chang, J.-C., Hsu, M.-Y., . . . Lin, H.-Y. (2022). White matter microstructural and morphometric alterations in autism: implications for intellectual capabilities. *Molecular Autism*, 13(1), 21. <https://doi.org/10.1186/s13229-022-00499-1>
- Zalesky, A., Fornito, A., & Bullmore, E. T. (2010). Network-based statistic: Identifying differences in brain networks. *NeuroImage*, 53(4), 1197–1207. <https://doi.org/10.1016/j.neuroimage.2010.06.041>
- Zhao, X., Li, Y., Tian, Q., Zhu, B., & Zhao, Z. (2019). Repetitive transcranial magnetic stimulation increases serum brain-derived neurotrophic factor and decreases interleukin-1 β and tumor necrosis factor- α in elderly patients with refractory depression. *Journal of International Medical Research*, 47(5), 1848–1855. <https://doi.org/10.1177/0300060518817417>

Publisher's Note Springer Nature remains neutral with regard to jurisdictional claims in published maps and institutional affiliations.

Springer Nature or its licensor (e.g. a society or other partner) holds exclusive rights to this article under a publishing agreement with the author(s) or other rightsholder(s); author self-archiving of the accepted manuscript version of this article is solely governed by the terms of such publishing agreement and applicable law.